Title

Near-continuous tremor and low-frequency earthquake activities in the Alaska-Aleutian subduction zone revealed by a mini seismic array

Journal

Geophysical Research Letters, 44(11)

ISSN

0094-8276

Authors

Li, Bo

Ghosh, Abhijit

Publication Date

2017-06-16

DOI

10.1002/2016gl072088

Peer reviewed

AGU PUBLICATIONS

Geophysical Research Letters

RESEARCH LETTER
10.1002/2016GL072088

Key Points:
- Tremor and LFEs occur daily in the Alaska-Aleutian subduction zone
- Tremor sources in this region are clustered in two patches with an ~25 km gap in between
- Tremor sources show migration patterns with both along strike and dip components with a wide range of velocities

Supporting Information:
- Supporting Information S1

Correspondence to:
B. Li,
bli017@ucr.edu

Citation:
Li, B., and A. Ghosh (2017), Near-continuous tremor and low-frequency earthquake activities in the Alaska-Aleutian subduction zone revealed by a mini seismic array, *Geophys. Res. Lett.*, *44*, doi:10.1002/2016GL072088.

Received 24 NOV 2016
Accepted 7 MAY 2017
Accepted article online 15 MAY 2017

Near-continuous tremor and low-frequency earthquake activities in the Alaska-Aleutian subduction zone revealed by a mini seismic array

Bo Li[1] **and Abhijit Ghosh**[1]

[1]Department of Earth Sciences, University of California, Riverside, California, USA

Abstract Tectonic tremor and low-frequency earthquakes (LFEs) are relatively poorly studied in the Alaska-Aleutian subduction zone due to the limited data availability, difficult logistics, and rugged terrain. Using 2 months of continuous data recorded by a mini seismic array in the Akutan Island, we detect near-continuous tremor activity with an average of 1.3 h of tectonic tremor per day using a beam backprojection method. Tremor sources are clustered in two patches with an ~25 km gap in between them. In addition, we visually identify three low-frequency earthquakes, and using them as templates, we detect ~1300 additional LFEs applying a matched-filter method. Tremor and LFE activities agree well in space and time, and LFEs show a much smaller recurrence interval during tremor than during non-tremor time periods. Tremor sources propagate both along the strike and dip directions of the subduction fault with velocities ranging between 13 and 110 km/h. Prolific patchy tremor and LFE activities suggest lateral heterogeneity in the locked to freely slipping transition zone, indicating that slow earthquakes may play an important role in the earthquake cycles in this subduction zone.

1. Introduction

Tectonic tremor (TT) or nonvolcanic tremor, low-frequency earthquakes (LFEs), very low frequency earthquakes, and episodic slow slip events (SSEs) are observed as coupled phenomena in many subduction zones, such as southwestern Japan, Cascadia, and Costa Rica [*Brown et al.*, 2009; *Ghosh et al.*, 2012, 2015; *Hutchison and Ghosh*, 2016; *Shelly et al.*, 2006]. Tremor event has been found to be triggered by stresses as low as a few kilopascals produced by tidal and dynamic stresses from passing teleseismic waves [*Ghosh et al.*, 2009; *Rubinstein et al.*, 2008; *Thomas et al.*, 2013]. Tremor activity is thought to represent slip on small asperities due to slow slip in the surrounding region [*Bartlow et al.*, 2011]. Therefore, migration directions, patterns, and speed of tremor sources may provide clues about the dynamics of the slow earthquakes and the rheological properties of the asperities on the subduction interface [*Ghosh et al.*, 2010a, 2010b; *Gershenzon et al.*, 2011; *Obara et al.*, 2011]. SSEs release accumulated plate boundary strain with durations on the order of days to years with no or little seismic radiation. Tremor event is typically known to occur during episodes of SSEs and located on fault segments downdip of the seismogenic zone [*Rogers and Dragert*, 2003; *Shelly et al.*, 2006]. LFEs are also thought to be generated by slip on relatively small asperities on the plate interface [*Ide et al.*, 2007a, 2007b; *Royer and Bostock*, 2014]. There is evidence that signals from LFEs comprise at least a portion of tremor, and the LFEs occur on the plate interface, coincident with the inferred zone of slow slip [*Frank et al.*, 2013, 2015; *Shelly et al.*, 2006, 2007b]. Thus, more detailed studies of tremor and LFEs in the subduction zones help better understand the subduction processes, fault dynamics, mechanism of tremor sources, constrain the depth of slow slip events, and delineate the transition zone and plate interface more accurately. Compared to other subduction zones, investigating tremor and LFEs along the Alaska-Aleutian subduction zone is more challenging due to the harsh weather conditions, limited land, sparse seismic station coverage, and the interference due to signals from volcanic activities.

The Alaska-Aleutian subduction zone is about 3800 km long and forms the plate boundary between the Pacific and North American plates [*Ruppert et al.*, 2007]. Convergence directions and velocities change along strike ranging between 5.1 and 7.5 cm/yr [*DeMets et al.*, 1994]. It is one of the most seismically and volcanically active subduction zones in the world. In the last 80 years, four large earthquakes with $M_w > 8$ have occurred: the 1938 M_w 8.2 Shumagin Islands, 1957 M_w 8.6 Andreanof Islands, 1964 M_w 9.2 Good Friday, and 1965 M_w 8.7 Rat Islands earthquakes [*Brown et al.*, 2013] (Figure 1). TT and LFEs have previously been identified in south central Alaska and along the Alaska-Aleutian Arc [*Brown et al.*, 2013; *Gomberg and Prejean*, 2013; *Peterson*

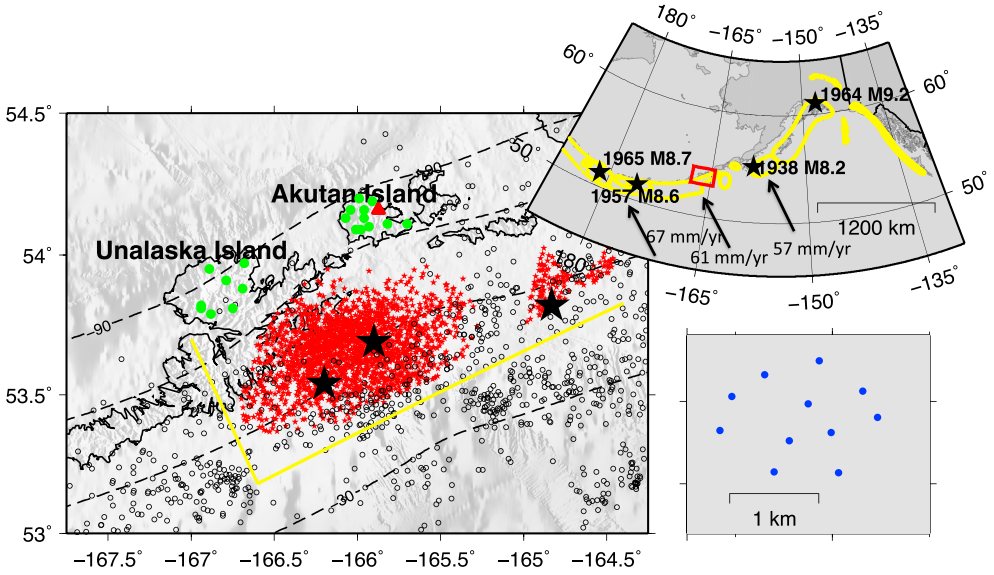

Figure 1. Tremor sources and LFEs distribution in the study region and historic large earthquakes in the Alaska-Aleutian subduction zone. Each red star represents the location of 1 min tremor signal determined by the beam backprojection method, and the black stars show three visually detected LFEs located using arrival times of body waves. The yellow lines AB and AC are used to calculate the along strike and along dip distances of tremor source migrations. The contour lines show the depth of the subduction interface according to the United States Geological Survey (USGS) slab model [*Hayes et al.*, 2012]. The black open circles show regular fast earthquakes (1 January 2002 to 10 January 2016) located near the subduction surface. They are taken from the Advanced National Seismic System (ANSS) catalog. The red triangle represents the mini array location, and the green dots show the Alaska Volcano Observatory (AVO) stations. The right bottom panel shows the distribution of the mini array stations. The right top figure shows the Alaska-Aleutian subduction zone, with the yellow dotted closed lines showing the rupture zones for larger earthquakes [*Brown et al.*, 2013]. The red box shows our study area, which is located along the eastern edge of the 1957 M 8.6 and to the west of the 1938 M_w 8.2 megathrust earthquakes.

et al., 2011]. Details of their spatiotemporal distribution, however, is poorly known due to limited number of tremor/LFE studies in this area.

Here we study the tremor and LFEs in the Akutan and Unalaska region using 2 months of high-quality continuous seismic data set recorded by a mini seismic array (array stations are distributed within a small aperture, a few kilometers) (Figure 1). We detect and locate tremor signals and LFEs, analyze their spatiotemporal distribution, and explore the relationship between them. In addition, we compare their locations with the rupture zone of the 1957 M_w 8.6 earthquake in this region. Finally, we discuss possible implications for the observed distribution of tremor and LFE sources in the study area.

2. Data and Method

In this study, we use data from a dense mini seismic array designed with 11 three-component stations deployed on Akutan Island in 2012. The array was operational for 2 months from early July to September. Array technique has been successfully applied to detect and locate tremor activity in Cascadia and along the San Andreas Fault [*Ghosh et al.*, 2012; *Ghosh*, 2014]. It is also logistically easier to deploy and service mini arrays as opposed to a conventional seismic network, which requires greater interspacing distance and aperture, particularly in the Alaska-Aleutian subduction zone due to its remoteness, rough, unpredictable weather, and challenging terrain.

For tremor signal detection and source location, we apply a beam backprojection method [*Ghosh et al.*, 2009, 2012] to automatically scan 2 months of seismic data collected by this mini array. Assuming that tremor source is occurring on the plate interface, we divide the interface into 0.02 by 0.02° grid points and calculate the slowness of each grid along the raypath to the array center with a velocity model for this area. Then the beam backprojection method traces the slowness calculated using the array data back to the slab interface to find the location of the signal. This method consistently detects a longer duration tremor signal than visual detection or envelope cross-correlation method in Cascadia subduction zone [*Ghosh et al.*, 2009, 2012]. We

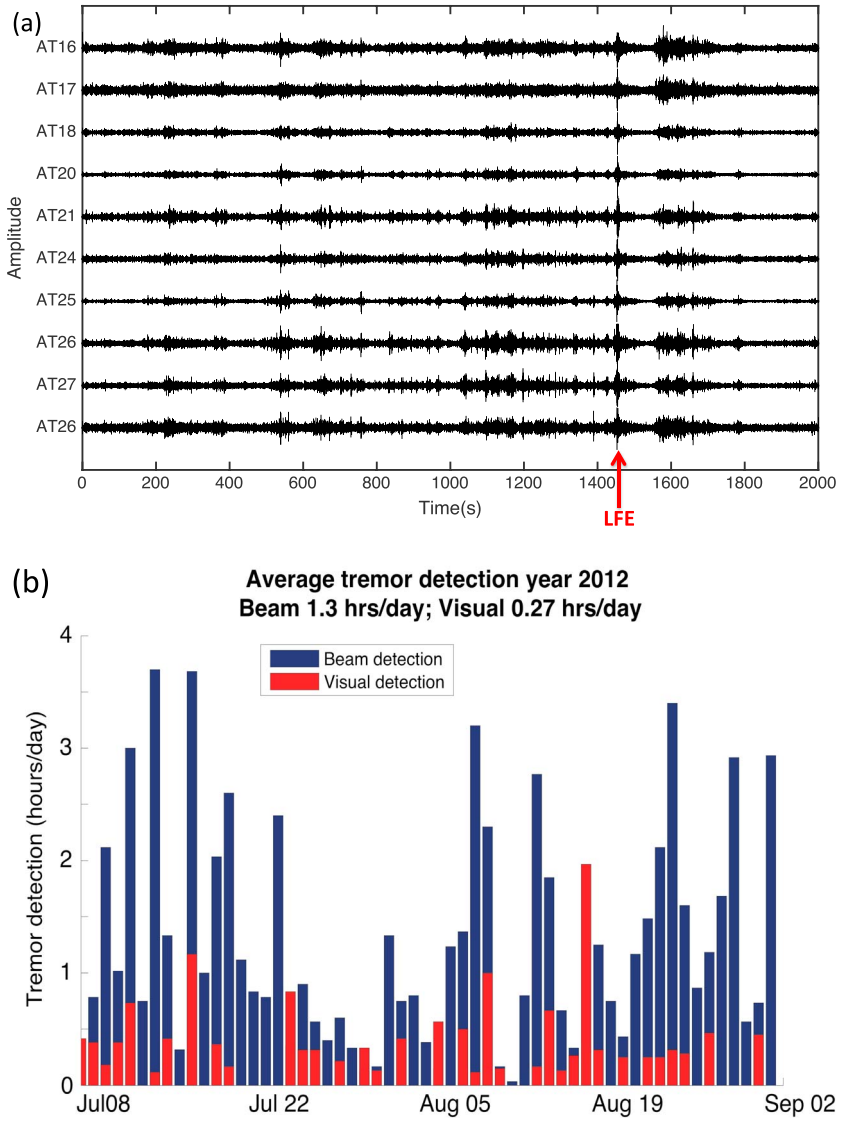

Figure 2. (a) Example of 2–8 Hz filtered velocity seismograms for the tremor activity on 23 July 2012, recorded by the mini array. The red arrow shows one of the visually identified LFE templates. (b) Tremor detection comparison using beam backprojection and visual scanning method. The beam backprojection method detects 5 times more duration of tremor activity compared to visual detection.

use the United States Geological Survey (USGS) slab model [*Hayes et al.*, 2012] as the subduction interface and a 1-D velocity model [*Fogleman et al.*, 1993] to locate the tremor sources. Then we discard spurious scattered sources (less than three counts in one grid region) using a clustering algorithm. After that, the tremor source locations are calibrated applying an empirical calibration function, which is calculated by analyzing regular earthquake signals recorded by the array [*Ghosh et al.*, 2012]. We compare the earthquake locations obtained by the beam backprojection method and the locations in the Advanced National Seismic System (ANSS) earthquake catalog. Then we determine a calibration function by minimizing the summed location differences. Finally, we calculate the location uncertainty for tremor sources. Average location uncertainty in NS is 3.51 km and EW is 3.78 km (Figure S1 in the supporting information). The frequency band of 2–6 Hz is used for the analyses of LFEs, and a slightly narrower band for tremor to separate tremor signals from noise.

For tremor, we use a 1 min independent (no overlap) sliding time window to determine its source location and migration patterns. The repeating LFEs are difficult to detect due to their inherently low signal-to-

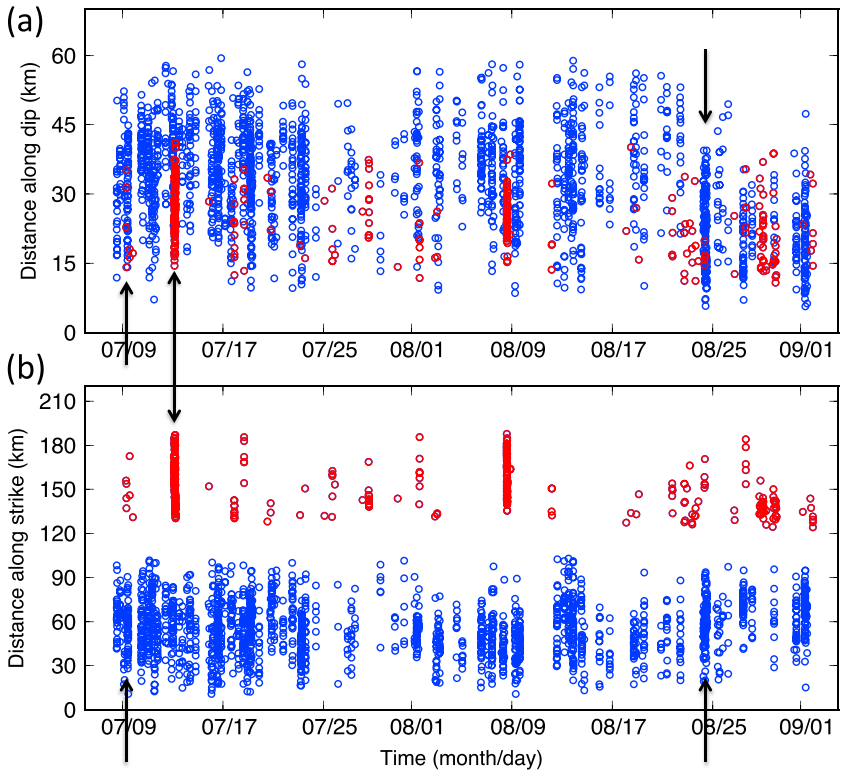

Figure 3. (a) Tremor source migrations along the strike relative to the reference line AB in Figure 1. Each circle represents the tremor source location that is determined by the beam backprojection method using a 1 min independent time window. Blue and red colors indicate the tremor source locations in western and eastern clusters, respectively. (b) Tremor sources migration along the dip direction using the reference line AC in Figure 1. Black arrows point to the tremor sources shown in Figure 4.

noise ratios (SNRs) [*Brown et al.*, 2008; *Shelly et al.*, 2006]. This problem can be circumvented once LFE templates are identified. Scanning 2 months of continuous seismic data, we visually identify three "clean" LFEs and use them as templates to search for additional LFEs that show similar waveforms across the array applying a matched-filter method. For each template, we use a sliding 6 s time window, with a 0.025 s time step to search this 2 months of continuous seismic data. Though it is difficult to distinguish *S* and *P* wave arrivals in an LFE at a single station due to low SNR, they become recognizable on aligned and stacked waveforms. We use both the mini array stations and the USGS-Alaska Volcano Observatory (AVO) stations to locate the LFE families using phase arrivals and the hypoinverse algorithm [*Klein*, 2002].

3. Results

3.1. Tectonic Tremor (TT)

The beam backprojection method results in significant improvements of tremor detection over the visual detection. During the time period of this study (2 months), the beam backprojection method detects tremor activity for a duration lasting 5 times longer than that detected by visual inspection (Figure 2). The beam backprojection method detects 1.3 h of tremor activity per day on average. In contrast, visual inspection reveals tremor activity of only 0.27 h per day on average. The duration of continuous tremor activity lasts from minutes to hours, and tremor sources show a spatiotemporally heterogeneous distribution in the study region (Figures 3 and S2).

The tremor source catalog produced using the beam backprojection method shows that the tremor sources are located to the south of the array in two clusters, with the majority of them distributed offshore to the south of the Unalaska and Akutan Islands. Assuming that the tremor is generated by slip on the subduction interface, the two clusters are located at a depth range between 45 and 70 km. This is deeper than the

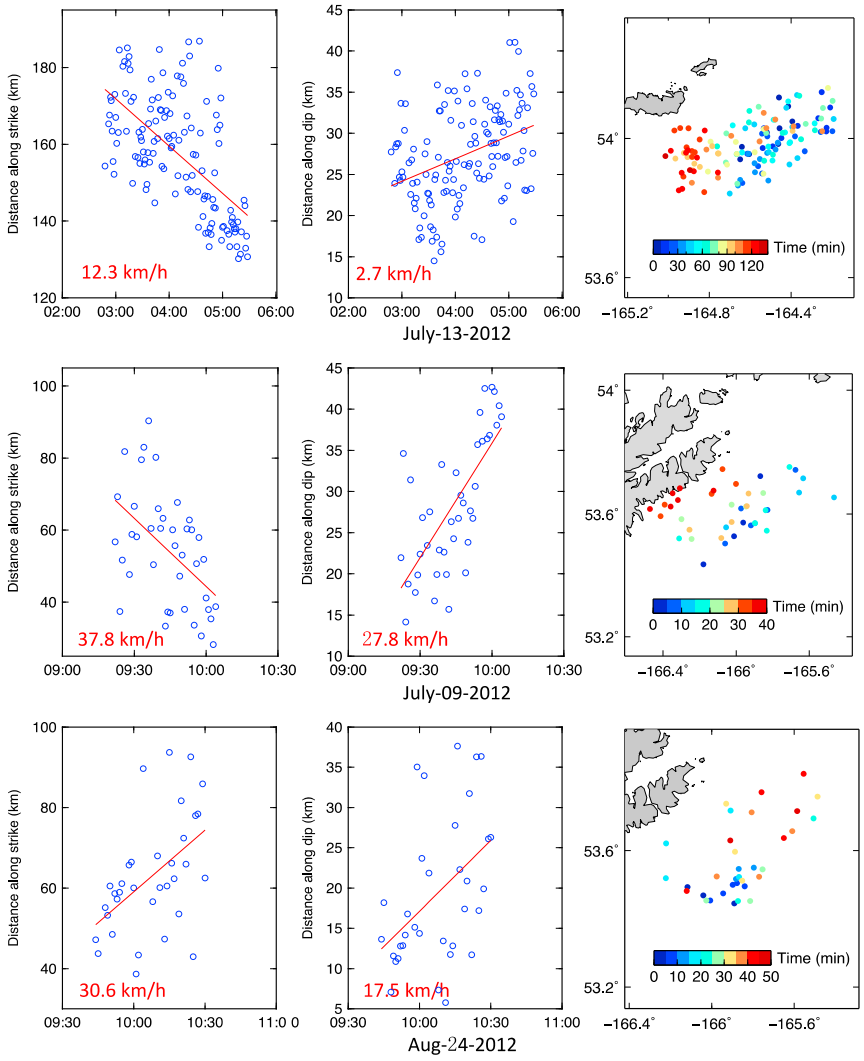

Figure 4. Different tremor source propagation patterns in the study region. Top row represents the tremor source propagation in the eastern cluster, and the middle and bottom rows show the tremor source propagations examples in the western cluster. The red lines represent the average velocity along dip and strike as delineated in Figure 1. The average velocities for each case are marked at the bottom left of the panels.

30–35 km depth range in SW Japan, and the 30–40 km depth range in northern Cascadia and Costa Rica [*Brown et al.*, 2009]. Tremor sources in the western patch show a larger depth variation than the eastern patch. Interestingly, the downdip edge becomes progressively shallower from west to the east (Figure 1). Tremor studies in western Japan suggest that tremor sources are located downdip of the rupture zones and outline the depth extent of extensive slip during large earthquakes [*Ide et al.*, 2007a, 2007b]. This relationship has also been observed near Kodiak Island, Alaska, where tremor activity and LFEs occur near the downdip extent of the 1964 M_w 9.2 Alaska earthquake [*Brown et al.*, 2013]. In our study region, the sources of tremor appear to be located downdip of the rupture zone of the 1957 M_w 8.6 earthquake (Figure S2).

Along strike, there is an approximately 25 km gap in between the two tremor source clusters. The western cluster aligns along strike to the south of the Unalaska-Akutan Island and covers much larger area in map view (Figures 1 and S2). On the other hand, the eastern cluster is much smaller and located to the southeast of the Akutan Island. The location density map shows more detailed pattern of spatial distribution, indicating that tremor sources are not uniformly distributed even in the same cluster (Figure S2). The majority of the tremor source locations are within a few discrete patches in the western cluster, with the most tremor-active patch just offshore the Unalaska Island.

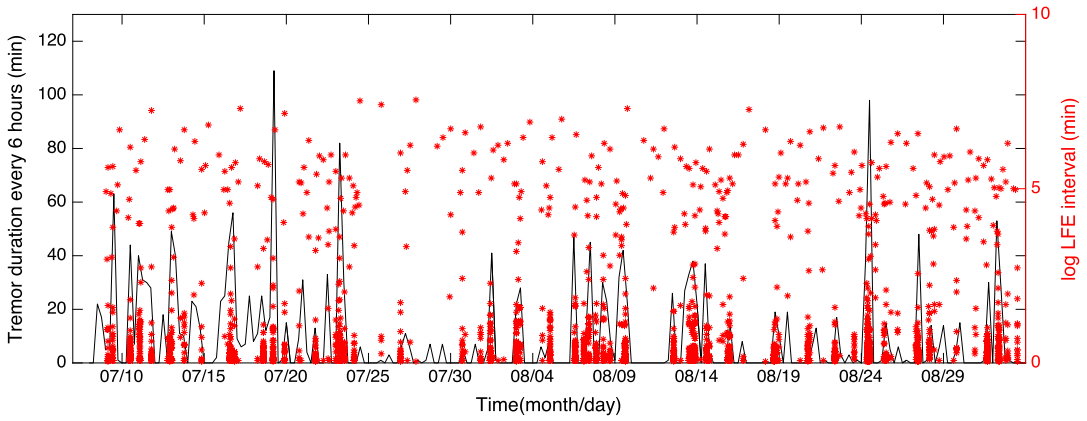

Figure 5. Tremor activity and the LFE recurrence intervals (in natural log scale). The black line shows the tremor duration every 6 h. The red star represents the recurrence interval between two successive LFEs.

Tremor in the western cluster is temporally more active and has a longer duration than that in the eastern cluster (Figure 3). Tremor in the eastern cluster is only active for a few times during this 2 month period, while the western cluster shows activity almost daily for the entire 2 months. Migration is one of the most important features of tremor sources. In the study region, tremor sources generally show along strike migration. In the eastern cluster, tremor sources propagate to the southwest along strike at a speed about 13–15 km/h (Figure 4), with only a small amount of along dip propagation (Figures 3 and 4). In the western patch, they move in both directions along strike, with a higher velocity (30–110 km/h), and show movements along both strike and dip directions (Figure 4).

3.2. Low-Frequency Earthquakes (LFEs)

The low SNR of LFEs makes it very difficult to detect and analyze an individual LFE event. Swarms of repeating LFEs have been observed within tremor, with each source producing many LFEs over time—known as multiplets [*Shelly et al*., 2007a, 2007ab]. We visually inspect seismic array data and identify three clean LFEs (Figure S3a) and use them as the templates to detect more repeating LFEs (Figure S3c). Using the detection threshold as 10 times of the root-mean-square (Figure S3b), we detect a total of ~1300 LFEs. Similar to the findings in the southwestern Japan, Cascadia, and Costa Rica [*Brown et al*., 2009], the majority of the LFE activities are observed when the rate of tremor is high (Figures 5 and S4) and show a short recurrence interval (time between two consecutive LFEs), even though they are detected using two very different and independent techniques. In contrast, only scattered LFEs are detected with long recurrence intervals during times of tremor quiescence. In total, there are about 15% of LFEs detected in the absence of tremor. All three LFEs are located using *P* and *S* arrival times observed in the array stations and stations in the local network (AVO) in Unalaska and Akutan Islands. They are located within the tremor source clusters. Two LFEs are located in the western cluster, and the other one is in the eastern cluster (Figure 1). The two western LFEs occur over the entire 2 months, while in the eastern cluster, only intermittent LFE activity is detected (Figure S4)—consistent with the tremor activities.

4. Discussions and Conclusions

The abundant tremor activities and spatiotemporal distribution of their sources in the Unalaska/Akutan region may indicate frictional properties of the plate interface changing from stick-slip to creeping in both the dip and lateral directions [*Rubin*, 2011; *Gomberg and Prejean*, 2013]. Tremor events are heterogeneously distributed at greater depths in the Unalaska-Akutan region compared to other subduction zones. They are located offshore and clustered to the south of the Islands. Heterogeneous distribution of tremorgenic area along strike and dip may be due to the temperature variations along the arc that controls the distribution of hydrous minerals releasing fluids [*Katsumata and Kamaya*, 2003] enabling tremor activity. The Alaska-Aleutian subduction zone shows higher heat flow near the surface in the western part [*Batir et al*., 2013]. In addition, both Makushin and Akutan volcanoes are active and closer to the western tremor source cluster. The volcanic activity requires the magma produced by partial melting below the surface. It needs the

water dehydrated from the subducting crust to contribute to flux melting of the mantle rock [*Charles and David*, 1996]. Thus, there might be higher fluid pressure in the subduction region near the volcanoes, and as a result, more frequent tremor activities in the western cluster.

There is an ~25 km gap between the two tremor source clusters. Two months is too small of a time period to gauge long-term tremor behavior, but if this gap is a temporally stable feature, it may indicate lateral heterogeneity in the transition zone. Tremor sources in the study region distribute roughly in a zone between the slightly coupled and the decoupled area of the plate based on geodetic models [*Cross and Freymueller*, 2008; *Freymueller et al.*, 2008]. It is possible that this gap represents a predominantly aseismic creeping zone releasing stress without much seismic radiation. Using the ANSS earthquake catalog, we compare the tremor source distribution with earthquakes near the subduction interface (<5 km) for the last 15 years (1 January 2002 to 10 January 2016) (Figure 1). Interestingly, earthquakes appear to be occurring along the edge of the tremor source clusters, possibly delineating the boundaries of transitional asperities in the study region.

Tremor source migration is an important feature of its tectonic behavior and reflects the dynamics of slow earthquakes. Tremor sources in the eastern cluster show along strike migration in one direction—southwest, at a relatively low velocity (~13 km/h). In contrast, tremor sources in the western cluster show southwest and northeast propagation at a higher velocity, with both along strike and dip movements. Larger spacing between tremor source asperities would slow down slow slip propagation, which presumably drives the tremor propagation, due to the presence of more steadily creeping area in between asperities. In the numerical model, *Nakata et al.* [2011] also show that larger spaces/gaps between tremor asperities would result in lower propagation velocities, consistent with our interpretation. Based on the tremor source density distribution, the area covering the western cluster may have more frequent asperities, again consistent with our interpretation.

The majority of the LFEs occur within the tremor activities and show a much shorter recurrence interval than the LFEs occurring in the non-tremor time periods. The LFEs in the western cluster are more active than that in the eastern cluster, which is consistent with the tremor activities in the study region. Additionally, all three LFEs are located within the tremor source patches. This supports the notion that LFEs comprise at least a portion of tremor [*Shelly et al.*, 2007b; *Brown et al.*, 2008]. In addition, there are some LFE activities that do not temporally coincide with tremor activities. This may be explained by the possible incomplete detection of tremor because of the limitation of the station distribution and low SNR. Similar phenomenon has been observed in Guerrero, Mexico, where only 18.3% of LFEs are reported to occur during tectonic tremor for a yearlong period [*Frank and Shapiro*, 2014; *Husker et al.*, 2012]. LFEs are considered small seismic events that occur at the fault releasing accumulated tectonic stress [*Ide et al.*, 2007a, 2007b; *Shelly et al.*, 2007a, 2007b; *Ohta and Ide*, 2011; *Bostock et al.*, 2012]. In addition, we calculated the relative moment of tremor sources by integrating the far-field displacement pulse [*Shearer*, 2009] and then corrected for distance from the source location to the array center. The result shows that more larger moment tremor events occur in the western cluster. Thus, more frequent activities of tremors and LFEs in the western region may suggest a higher seismic slip rate than that in the eastern region.

In conclusions, the beam backprojection method shows high capability of tremor detection and spatial resolution in locating tremor in the Unalaska-Akutan subduction zone. The near-continuous tremor activity is clustered in two patches. The western patch has a larger depth range and shows higher tremor source propagation velocities. There is an ~25 km gap between the two tremor source clusters, possibly indicating lateral heterogeneity in the transition zone. Regular earthquakes are located along the edges of the tremor source patches possibly delineating the boundaries of the tremorgenic transition zone. The spatial and temporal distributions of LFE and tremor activity coincide with one another. More frequent tremor events and LFEs in the western patch may be a result of higher fluid activity and indicate a higher seismic slip rate than the eastern region.

Acknowledgments

This project is supported by the National Science Foundation-Division of Earth Sciences awards 1358686, 1620655, and 1135455; EarthScope; the United States Geological Survey; the Alaska Volcano Observatory; and the Southern California Earthquake Center. We are grateful to Stephanie Prejean, Matt Haney, and John Power for their help in fieldwork and logistics. The Alaska Volcano Observatory stations data are provided by the Incorporated Research Institutions for Seismology (IRIS) (http://ds.iris.edu/gmap/AV). The authors would like to thank the UCR Seismology group and Kenny Ryan for their suggestions. We also want to extend our thanks to two anonymous reviewers for their constructive comments that helped improve the content of this manuscript. All the figures are made using Generic Mapping Tools [*Wessel and Smith*, 1991].

References

Bartlow, N. M., S. Miyazaki, A. M. Bradley, and P. Segall (2011), Space-time correlation of slip and tremor during the 2009 Cascadia slow slip event, *Geophys. Res. Lett.*, *38*, L18309, doi:10.1029/2011GL048714.

Batir, J. F., D. D. Blackwell, and M. C. Richards (2013), Updated surface heat flow map of Alaska, *GRC Trans.*, *37*, 2013.

Bostock, M. G., A. A. Royer, E. H. Hearn, and S. M. Peacock (2012), Low frequency earthquakes below southern Vancouver Island, *Geochem. Geophys. Geosyst.*, *13*, Q11007, doi:10.1029/2012GC004391.

Brown, J. R., G. C. Beroza, and D. R. Shelly (2008), An autocorrelation method to detect low frequency earthquakes within tremor, *Geophys. Res. Lett.*, *35*, L16305, doi:10.1029/2008GL034560.

Brown, J. R., G. C. Beroza, S. Ide, K. Ohta, D. R. Shelly, S. Y. Schwartz, W. Rabbel, M. Thorwart, and H. Kao (2009), Deep low-frequency earthquakes in tremor localize to the plate interface in multiple subduction zones, *Geophys. Res. Lett.*, *36*, L19306, doi:10.1029/2009GL040027.

Brown, J. R., S. G. Prejean, G. C. Beroza, J. Gomberg, and P. J. Haeussler (2013), Deep low-frequency earthquakes in tectonic tremor along the Alaska-Aleutian subduction zone, *J. Geophys. Res. Solid Earth*, *118*, 1079–1090, doi:10.1029/2012JB009459.

Charles, C. P., and M. David (1996), Physical Geology, 7th ed., pp. 88-89, Wm. C. Brown Publ., Dubuque, Iowa.

Cross, R. S., and J. T. Freymueller (2008), Evidence for and implications of a Bering plate based on geodetic measurements from the Aleutians and western Alaska, *J. Geophys. Res.*, *113*, B07405, doi:10.1029/2007JB005136.

DeMets, C., R. G. Gordon, D. F. Argus, and S. Stein (1994), Effects of recent revisions to the geomagnetic reversal time scale on estimates of current plate motions, *Geophys. Res. Lett.*, *21*, 2191–2194, doi:10.1029/94GL02118.

Fogleman, K. A., J. C. Lahr, C. D. Stephens, and R. A. Page (1993, revised 2012), Earthquake locations determined by the southern Alaska seismograph network for October 1971 through May 1989, *U.S. Geol. Surv. Open File Rep., 93-309*, Version 1.1, 54 pp.

Frank, W. B., and N. M. Shapiro (2014), Automatic detection of low-frequency earthquakes (LFEs) based on a beamformed network response, *Geophys. J. Int.*, *197*(2), 1215–1223, doi:10.1093/gji/ggu058.

Frank, W. B., N. M. Shapiro, V. Kostoglodov, A. L. Husker, M. Campillo, J. S. Payero, and G. A. Prieto (2013), Low-frequency earthquakes in the Mexican sweet spot, *Geophys. Res. Lett.*, *40*, 2661–2666, doi:10.1002/grl.50561.

Frank, W. B., N. M. Shapiro, A. L. Husker, V. Kostoglodov, H. S. Bhat, and M. Campillo (2015), Along-fault pore-pressure evolution during a slow-slip event in Guerrero, Mexico, *Earth Planet. Sci. Lett.*, *413*, 135–143, doi:10.1016/j.epsl.2014.12.051.

Freymueller, J. T., S. C. Cohen, R. Cross, J. Elliott, H. J. Fletcher, S. Hreinsdottir, C. F. Larsen, and C. Zweck (2008), Active deformation processes in Alaska, based on 15 years of GPS measurements, in *Geophys. Monogr. Ser.*, vol. 179, edited by J. T. Freymueller et al., pp. 1–42, AGU, Washington, D. C.

Gershenzon, N. I., G. Bambakidis, E. Hauser, A. Ghosh, and K. C. Creager (2011), Episodic tremors and slip in Cascadia in the framework of the Frenkel-Kontorova model, *Geophys. Res. Lett.*, *38*, L01309, doi:10.1029/2010GL045225.

Ghosh, A., E. Huesca-Pérez, E. E. Brodsky, and Y. Ito (2015), Very low frequency earthquakes in Cascadia migrate with tremor, *Geophys. Res. Lett.*, *42*, 3228–3232, doi:10.1002/2015GL063286.

Ghosh, A., J. E. Vidale, J. R. Sweet, K. C. Creager, and A. G. Wech (2009), Tremor patches in Cascadia revealed by seismic array analysis, *Geophys. Res. Lett.*, *36*, L17316, doi:10.1029/2009GL039080.

Ghosh, A., J. E. Vidale, J. R. Sweet, K. C. Creager, A. G. Wech, and H. Houston (2010a), Tremor bands sweep Cascadia, *Geophys. Res. Lett.*, *37*, L08301, doi:10.1029/2009GL042301.

Ghosh, A., J. E. Vidale, J. R. Sweet, K. C. Creager, A. G. Wech, H. Houston, and E. E. Brodsky (2010b), Rapid, continuous streaking of tremor in Cascadia, *Geochem. Geophys. Geosyst.*, *11*, Q12010, doi:10.1029/2010GC003305.

Ghosh, A., J. E. Vidale, and K. C. Creager (2012), Tremor asperities in the transition zone control evolution of slow earthquakes, *J. Geophys. Res.*, *117*, B10301, doi:10.1029/2012JB009249.

Ghosh, A., (2014), Revisiting tremor under the San Andreas Fault: An enhanced look through a mini seismic array near Parkfield, Presentation at the SCEC Annual Meeting 2014, abstract 191, Palm Springs, Calif.

Gomberg, J., and S. Prejean (2013), Triggered tremor sweet spots in Alaska, *J. Geophys. Res. Solid Earth*, *118*, 6203–6218, doi:10.1002/2013JB010273.

Hayes, G. P., D. J. Wald, and R. L. Johnson (2012), Slab1.0: A three-dimensional model of global subduction zone geometries, *J. Geophys. Res.*, *117*, B01302, doi:10.1029/2011JB008524.

Husker, A. L., V. Kostoglodov, V. M. Cruz-Atienza, D. Legrand, N. M. Shapiro, J. S. Payero, M. Campillo, and E. Huesca-Pérez (2012), Temporal variations of non-volcanic tremor (NVT) locations in the Mexican subduction zone: Finding the NVT sweet spot, *Geochem. Geophys. Geosyst.*, *13*, Q03011, doi:10.1029/2011GC003916.

Hutchison, A. A., and A. Ghosh (2016), Very low frequency earthquakes spatiotemporally asynchronous with strong tremor during the 2014 episodic tremor and slip event in Cascadia, *Geophys. Res. Lett.*, *43*, 6876–6882, doi:10.1002/2016GL069750.

Ide, S., G. C. Beroza, D. R. Shelly, and T. Uchide (2007a), A scaling law for slow earthquakes, *Nature*, *447*, 76–79, doi:10.1038/nature05780.

Ide, S., D. R. Shelly, and G. C. Beroza (2007b), Mechanism of deep low frequency earthquakes: Further evidence that deep non-volcanic tremor is generated by shear slip on the plate interface, *Geophys. Res. Lett.*, *34*, L03308, doi:10.1029/2006GL028890.

Katsumata, A., and N. Kamaya (2003), Low-frequency continuous tremor around the Moho discontinuity away from volcanoes in the southwest Japan, *Geophys. Res. Lett.*, *30*(1), 1020, doi:10.1029/2002GL015981.

Klein, F. W. (2002), User's guide to HYPOINVERSE-2000: A Fortran program to solve for earthquake locations and magnitudes, *U.S. Geol. Surv. Open File Rep., 02-172*, 123 pp., Menlo Park, Calif.

Nakata, R., R. Ando, T. Hori, and S. Ide (2011), Generation mechanism of slow earthquakes: Numerical analysis based on a dynamic model with brittle-ductile mixed fault heterogeneity, *J. Geophys. Res.*, *116*, B08308, doi:10.1029/2010JB008188.

Obara, K., T. Matsuzawa, S. Tanaka, T. Kimura, and T. Maeda (2011), Migration properties of non-volcanic tremor in Shikoku, southwest Japan, *Geophys. Res. Lett.*, *38*, L09311, doi:10.1029/2011GL047110.

Ohta, K., and S. Ide (2011), Precise hypocenter distribution of deep low-frequency earthquakes and its relationship to the local geometry of the subducting plate in the Nankai subduction zone, Japan, *J. Geophys. Res.*, *116*, B01308, doi:10.1029/2010JB007857.

Peterson, C. L., S. R. McNutt, and D. H. Christensen (2011), Nonvolcanic tremor in the Aleutian Arc, *Bull. Seismol. Soc. Am.*, *101*, 3081–3087.

Rogers, G., and H. Dragert (2003), Episodic tremor and slip on the Cascadia subduction zone: The chatter of silent slip, *Science*, *300*, 1942–1943, doi:10.1126/science.1084783.

Royer, A. A., and M. G. Bostock (2014), A comparative study of low frequency earthquake templates in northern Cascadia, *Earth Planet. Sci. Lett.*, *402*, 247–256.

Rubin, A. M. (2011), Designer friction laws for bimodal slow slip propagation speeds, *Geochem. Geophys. Geosyst.*, *12*, Q04007, doi:10.1029/2010GC003386.

Rubinstein, J. L., M. La Rocca, J. E. Vidale, K. C. Creager, and A. G. Wech (2008), Tidal modulation of nonvolcanic tremor, *Science*, *319*, 186–189, doi:10.1126/science.1150558.

Ruppert, N. A., J. M. Lees, and N. P. Kozyreva (2007), Seismicity, earthquakes and rupture along the Alaska-Aleutian and Kamchatka-Kurile subduction zones: A review, in *Volcanism and Subduction: The Kamchatka Region*, *Geophys. Monogr. Ser.*, vol. 172, edited by J. Eichelberger et al., pp. 129–144, AGU, Washington, D. C.

Shearer, P. M. (2009), *Introduction to Seismology*, 2nd ed., pp. 260–262, Cambridge Univ. Press, Cambridge.
Shelly, D. R., G. C. Beroza, S. Ide, and S. Nakamura (2006), Low-frequency earthquakes in Shikoku, Japan, and their relationship to episodic tremor and slip, *Nature*, *442*, 188–191, doi:10.1038/nature04931.
Shelly, D. R., G. C. Beroza, and S. Ide (2007a), Non-volcanic tremor and low-frequency earthquake swarms, *Nature*, *446*, 305–307, doi:10.1038/nature05666.
Shelly, D. R., G. C. Beroza, and S. Ide (2007b), Complex evolution of transient slip derived from precise tremor locations in western Shikoku, Japan, *Geochem. Geophys. Geosyst.*, *8*, Q10014, doi:10.1029/2007GC001640.
Thomas, T. W., J. E. Vidale, H. Houston, K. C. Creager, J. R. Sweet, and A. Ghosh (2013), Evidence for tidal triggering of high-amplitude rapid tremor reversals and tremor streaks in northern Cascadia, *Geophys. Res. Lett.*, *40*, 4254–4259, doi:10.1002/grl.50832.
Wessel, P. and W. H. F. Smith (1991), Free software helps map and display data, *Eos Trans., AGU*, *72*, 441–446.